Two Routes to Scalable Credit Assignment without Weight Symmetry

Daniel Kunin [*1] **Aran Nayebi** [*2] **Javier Sagastuy-Brena** [*1]
Surya Ganguli [3] **Jonathan M. Bloom** [4 5] **Daniel L. K. Yamins** [6 7 8]

Abstract

The neural plausibility of backpropagation has long been disputed, primarily for its use of non-local weight transport — the biologically dubious requirement that one neuron instantaneously measure the synaptic weights of another. Until recently, attempts to create local learning rules that avoid weight transport have typically failed in the large-scale learning scenarios where backpropagation shines, e.g. ImageNet categorization with deep convolutional networks. Here, we investigate a recently proposed local learning rule that yields competitive performance with backpropagation and find that it is highly sensitive to metaparameter choices, requiring laborious tuning that does not transfer across network architecture. Our analysis indicates the underlying mathematical reason for this instability, allowing us to identify a more robust local learning rule that better transfers without metaparameter tuning. Nonetheless, we find a performance and stability gap between this local rule and backpropagation that widens with increasing model depth. We then investigate several non-local learning rules that relax the need for instantaneous weight transport into a more biologically-plausible "weight estimation" process, showing that these rules match state-of-the-art performance on deep networks and operate effectively in the presence of noisy updates. Taken together, our results suggest two routes towards the discovery of neural implementations for credit assignment without weight symmetry: further improvement of local rules so that they perform consistently across architectures and the identification of biological implementations for non-local learning mechanisms.

1. Introduction

Backpropagation is the workhorse of modern deep learning and the only known learning algorithm that allows multilayer networks to train on large-scale tasks. However, any exact implementation of backpropagation is inherently non-local, requiring instantaneous weight transport in which backward error-propagating weights are the transpose of the forward inference weights. This violation of locality is biologically suspect because there are no known neural mechanisms for instantaneously coupling distant synaptic weights. Recent approaches such as feedback alignment (Lillicrap et al., 2016) and weight mirror (Akrout et al., 2019) have identified circuit mechanisms that seek to approximate backpropagation while circumventing the weight transport problem. However, these mechanisms either fail to operate at large-scale (Bartunov et al., 2018) or, as we demonstrate, require complex and fragile metaparameter scheduling during learning. Here we present a unifying framework spanning a space of learning rules that allows for the systematic identification of robust and scalable alternatives to backpropagation.

To motivate these rules, we replace tied weights in backpropagation with a regularization loss on untied forward and backward weights. The forward weights parametrize the global cost function, the backward weights specify a descent direction, and the regularization constrains the relationship between forward and backward weights. As the system iterates, forward and backward weights dynamically align, giving rise to a pseudogradient. Different regularization terms are possible within this framework. Critically, these regularization terms decompose into geometrically natural primitives, which can be parametrically recombined to construct a diverse space of credit assignment strategies. This space encompasses existing approaches (including feedback alignment and weight mirror), but also elucidates novel learning rules. We show that several of these new strategies

[*]Equal contribution [1]Institute for Computational and Mathematical Engineering, Stanford University [2]Neurosciences PhD Program, Stanford University [3]Department of Applied Physics, Stanford University [4]Broad Institute of MIT and Harvard, Cambridge, MA [5]Cellarity, Cambridge, MA [6]Department of Psychology, Stanford University [7]Department of Computer Science, Stanford University [8]Wu Tsai Neurosciences Institute, Stanford University. Correspondence to: Aran Nayebi <anayebi@stanford.edu>, Daniel Kunin <kunin@stanford.edu>, Javier Sagastuy-Brena <jvrsgsty@stanford.edu>.

Proceedings of the 37^{th} International Conference on Machine Learning, Online, PMLR 119, 2020.

are competitive with backpropagation on real-world tasks (unlike feedback alignment), without the need for complex metaparameter tuning (unlike weight mirror). These learning rules can thus be easily deployed across a variety of neural architectures and tasks. Our results demonstrate how high-dimensional error-driven learning can be robustly performed in a biologically motivated manner.

2. Related Work

Soon after Rumelhart et al. (1986) published the backpropagation algorithm for training neural networks, its plausibility as a learning mechanism in the brain was contended (Crick, 1989). The main criticism was that backpropagation requires exact transposes to propagate errors through the network and there is no known physical mechanism for such an "operation" in the brain. This is known as the *weight transport problem* (Grossberg, 1987). Since then many credit assignment strategies have proposed circumventing the problem by introducing a distinct set of feedback weights to propagate the error backwards. Broadly speaking, these proposals fall into two groups: those that encourage symmetry between the forward and backward weights (Lillicrap et al., 2016; Nøkland, 2016; Bartunov et al., 2018; Liao et al., 2016; Xiao et al., 2019; Moskovitz et al., 2018; Akrout et al., 2019), and those that encourage preservation of information between neighboring network layers (Bengio, 2014; Lee et al., 2015; Bartunov et al., 2018).

The latter approach, sometimes referred to as target propagation, encourages the backward weights to locally invert the forward computation (Bengio, 2014). Variants of this approach such as difference target propagation (Lee et al., 2015) and simplified difference target propagation (Bartunov et al., 2018) differ in how they define this inversion property. While some of these strategies perform well on shallow networks trained on MNIST and CIFAR10, they fail to scale to deep networks trained on ImageNet (Bartunov et al., 2018).

A different class of credit assignment strategies focuses on encouraging or enforcing symmetry between the weights, rather than preserving information. Lillicrap et al. (2016) introduced a strategy known as feedback alignment in which backward weights are chosen to be fixed random matrices. Empirically, during learning, the forward weights partially align themselves to their backward counterparts, so that the latter transmit a meaningful error signal. Nøkland (2016) introduced a variant of feedback alignment where the error signal could be transmitted across long range connections. However, for deeper networks and more complex tasks, the performance of feedback alignment and its variants break down (Bartunov et al., 2018).

Liao et al. (2016) and Xiao et al. (2019) took an alternative route to relaxing the requirement for exact weight symmetry by transporting just the sign of the forward weights during learning. Moskovitz et al. (2018) combined sign-symmetry and feedback alignment with additional normalization mechanisms. These methods outperform feedback alignment on scalable tasks, but still perform far worse than backpropagation. It is also not clear that instantaneous sign transport is more biologically plausible than instantaneous weight transport.

More recently, Akrout et al. (2019) introduced weight mirror (WM), a learning rule that incorporates dynamics on the backward weights to improve alignment throughout the course of training. Unlike previous methods, weight mirror achieves backpropagation level performance on ResNet-18 and ResNet-50 trained on ImageNet.

Concurrently, Kunin et al. (2019) suggested training the forward and backward weights in each layer as an encoder-decoder pair, based on their proof that L_2-regularization induces symmetric weights for linear autoencoders. This approach incorporates ideas from both information preservation and weight symmetry.

A complementary line of research (Xie & Seung, 2003; Scellier & Bengio, 2017; Bengio et al., 2017; Guerguiev et al., 2017; Whittington & Bogacz, 2017; Sacramento et al., 2018; Guerguiev et al., 2019) investigates how learning rules, even those that involve weight transport, could be implemented in a biologically mechanistic manner, such as using spike-timing dependent plasticity rules and obviating the need for distinct phases of training. In particular, Guerguiev et al. (2019) show that key steps in the Kunin et al. (2019) regularization approach could be implemented by a spike-based mechanism for approximate weight transport.

In this work, we extend this regularization approach to formulate a more general framework of credit assignment strategies without weight symmetry, one that encompasses existing and novel learning rules. Our core result is that the best of these strategies are substantially more robust across architectures and metaparameters than previous proposals.

3. Regularization Inspired Learning Rule Framework

We consider the credit assignment problem for neural networks as a layer-wise regularization problem. We consider a network parameterized by forward weights θ_f and backward weights θ_b. Informally, the network is trained on the sum of a global task function $\mathcal{J}$ and a layer-wise regularization function[1] $\mathcal{R}$:

$$\mathcal{L}(\theta_f, \theta_b) = \mathcal{J}(\theta_f) + \mathcal{R}(\theta_b).$$

[1] $\mathcal{R}$ is not regularization in the traditional sense, as it does not directly penalize the forward weights θ_f from the cost function $\mathcal{J}$.

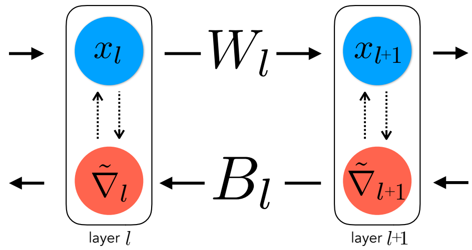

Figure 1. **Notational diagram.** The forward weight W_l propagates the input signal x_l downstream through the network. The backward weight B_l propagates the pseudogradient $\widetilde{\nabla}_{l+1}$ of $\mathcal{J}$ upstream through the network. The regularization function $\mathcal{R}$ is constructed layer-wise from x_l, x_{l+1}, W_l and B_l. Similar to Akrout et al. (2019), we assume lateral pathways granting the backward weights access to x and the forward weights access to $\widetilde{\nabla}$. Biases and non-linearities are omitted from the diagram.

Formally, every step of training consists of two updates, one for the forward weights and one for the backward weights. The forward weights are updated according to the error signal on $\mathcal{J}$ propagated through the network by the backward weights, as illustrated in Fig. 1. The backward weights are updated according to gradient descent on $\mathcal{R}$.

$$\Delta\theta_f \propto \widetilde{\nabla} J \qquad \Delta\theta_b \propto \nabla R$$

Thus, $\mathcal{R}$ is responsible for introducing dynamics on the backward weights, which in turn impacts the dynamics of the forward weights. The functional form of $\mathcal{R}$ gives rise to different learning rules and in particular the locality of a given learning rule depends solely on the locality of the computations involved in $\mathcal{R}$.

3.1. Regularization Primitives

In this work, the regularization function $\mathcal{R}$ is built from a set of simple *primitives* $\mathcal{P}$, which at any given layer l are functions of the forward weight $W_l \in \theta_f$, backward weight $B_l \in \theta_b$, layer input x_l, and layer output x_{l+1} as depicted in Fig. 1. These primitives are biologically motivated components with strong geometric interpretations, from which more complex learning rules may be algebraically constructed.

The primitives we use, displayed in Table 1, can be organized into two groups: those that involve purely local operations and those that involve at least one non-local operation. To classify the primitives, we use the criteria for locality described in Whittington & Bogacz (2017): (1) *Local computation*. Computations only involve synaptic weights acting on their associated inputs. (2) *Local plasticity*. Weight modifications only depend on pre-synaptic and post-synaptic activity. A primitive is local if it satisfies both of these constraints and non-local otherwise.

We introduce three **local primitives**: $\mathcal{P}^{\text{decay}}$, $\mathcal{P}^{\text{amp}}$, and $\mathcal{P}^{\text{null}}$. The *decay* primitive can be understood as a form of energy efficiency penalizing the Euclidean norm of the backward weights. The *amp* primitive promotes alignment of the layer input x_l with the reconstruction $B_l x_{l+1}$. The *null* primitive imposes sparsity in the layer-wise activity through a Euclidean norm penalty on the reconstruction $B_l x_{l+1}$.

Local	$\mathcal{P}_l$	$\nabla\mathcal{P}_l$
decay	$\frac{1}{2}\|\|B_l\|\|^2$	B_l
amp	$-\text{tr}(x_l^\intercal B_l x_{l+1})$	$-x_l x_{l+1}^\intercal$
null	$\frac{1}{2}\|\|B_l x_{l+1}\|\|^2$	$B_l x_{l+1} x_{l+1}^\intercal$
Non-local	$\mathcal{P}_l$	$\nabla\mathcal{P}_l$
sparse	$\frac{1}{2}\|\|x_l^\intercal B_l\|\|^2$	$x_l x_l^\intercal B_l$
self	$-\text{tr}(B_l W_l)$	$-W_l^\intercal$

Table 1. **Regularization primitives.** Mathematical expressions for local and non-local primitives and their gradients with respect to the backward weight B_l. Note, both x_l and x_{l+1} are the post-nonlinearity rates of their respective layers.

We consider two **non-local primitives**: $\mathcal{P}^{\text{sparse}}$ and $\mathcal{P}^{\text{self}}$. The *sparse* primitive promotes energy efficiency by penalizing the Euclidean norm of the activation $x_l^\intercal B_l$. This primitive fails to meet the *local computation* constraint, as B_l describes the synaptic connections from the $l+1$ layer to the l layer and therefore cannot operate on the input x_l.

The *self* primitive promotes alignment of the forward and backward weights by directly promoting their inner product. This primitive fails the *local plasticity* constraint, as its gradient necessitates that the backward weights can exactly measure the strengths of their forward counterparts.

3.2. Building Learning Rules from Primitives

These simple primitives can be linearly combined to encompass existing credit assignment strategies, while also elucidating natural new approaches.

Feedback alignment (FA) (Lillicrap et al., 2016) corresponds to no regularization, $\mathcal{R}_{\text{FA}} \equiv 0$, effectively fixing the backward weights at their initial random values[2].

The **weight mirror (WM)** (Akrout et al., 2019) update, $\Delta B_l = \eta x_l x_{l+1}^\intercal - \lambda_{\text{WM}} B_l$, where η is the learning rate and λ_{WM} is a weight decay constant, corresponds to gradient descent on the layer-wise regularization function

$$\mathcal{R}_{\text{WM}} = \sum_{l \in \text{layers}} \alpha\mathcal{P}_l^{\text{amp}} + \beta\mathcal{P}_l^{\text{decay}},$$

for $\alpha = 1$ and $\beta = \frac{\lambda_{\text{WM}}}{\eta}$.

[2]We explore the consequences of this interpretation analytically in Appendix D.2.

	Alignment	$\mathcal{P}^{\text{decay}}$	$\mathcal{P}^{\text{amp}}$	$\mathcal{P}^{\text{null}}$	$\mathcal{P}^{\text{sparse}}$	$\mathcal{P}^{\text{self}}$
Local	Feedback					
	Weight Mirror	✓	✓			
	Information	✓	✓	✓		
Non-Local	Symmetric	✓				✓
	Activation		✓		✓	

Table 2. **Taxonomy of learning rules** based on the locality and composition of their primitives.

If we consider primitives that are functions of the pseudogradients $\widetilde{\nabla}_l$ and $\widetilde{\nabla}_{l+1}$, then the **Kolen-Pollack (KP)** algorithm, originally proposed by Kolen & Pollack (1994) and modified by Akrout et al. (2019), can be understood in this framework as well. See Appendix D.3 for more details.

The range of primitives also allows for learning rules not yet investigated in the literature. In this work, we introduce several such novel learning rules, including Information Alignment (IA), Symmetric Alignment (SA), and Activation Alignment (AA). Each of these strategies is defined by a layer-wise regularization function composed from a linear combination of the primitives (Table 2). Information Alignment is a purely local rule, but unlike feedback alignment or weight mirror, contains the additional null primitive. In §4, we motivate this addition theoretically, and show empirically that it helps make IA a higher-performing and substantially more stable learning rule than previous local strategies. SA and AA are both non-local, but as shown in §5 perform even more robustly than any local strategy we or others have found, and may be implementable by a type of plausible biological mechanism we call "weight estimation."

3.3. Evaluating Learning Rules

For all the learning rules, we evaluate two desirable target metrics.

Task Performance. Performance-optimized CNNs on ImageNet provide the most effective quantitative description of neural responses of cortical neurons throughout the primate ventral visual pathway (Yamins et al., 2014; Cadena et al., 2019), indicating the biological relevance of task performance. Therefore, our first desired target will be ImageNet top-1 validation accuracy, in line with Bartunov et al. (2018).

Metaparameter Robustness. Extending the proposal of Bartunov et al. (2018), we also consider whether a proposed learning rule's metaparameters, such as learning rate and batch size, transfer across architectures. Specifically, when we optimize for metaparameters on a given architecture (e.g. ResNet-18), we will fix these metaparameters and use them to train both deeper (e.g. ResNet-50) and different variants (e.g. ResNet-v2). Therefore, our second desired target will be ImageNet top-1 validation accuracy *across* models for *fixed* metaparameters.

4. Local Learning Rules

Instability of Weight Mirror. Akrout et al. (2019) report that the weight mirror update rule matches the performance of backpropagation on ImageNet categorization. The procedure described in Akrout et al. (2019) involves not just the weight mirror rule, but a number of important additional training details, including alternating learning modes and using layer-wise Gaussian input noise. After reimplementing this procedure in detail, and using their prescribed metaparameters for the ResNet-18 architecture, the best top-1 validation accuracy we were able to obtain was 63.5% ($\mathcal{R}_{\text{WM}}$ in Table 3), substantially below the reported performance of 69.73%. To try to account for this discrepancy, we considered the possibility that the metaparameters were incorrectly set. We thus performed a large-scale metaparameter search over the continuous α, β, and the standard deviation σ of the Gaussian input noise, jointly optimizing these parameters for ImageNet validation set performance using a Bayesian Tree-structured Parzen Estimator (TPE) (Bergstra et al., 2011). After considering 824 distinct settings (see Appendix B.1 for further details), the optimal setting achieved a top-1 performance of 64.07% ($\mathcal{R}_{\text{WM}}^{\text{TPE}}$ in Table 3), still substantially below the reported performance in Akrout et al. (2019).

Considering the second metric of robustness, we found that the WM learning rule is very sensitive to metaparameter tuning. Specifically, when using either the metaparameters prescribed for ResNet-18 in Akrout et al. (2019) or those from our metaparameter search, directly attempting to train other network architectures failed entirely (Fig. 3, brown line).

Why is weight mirror under-performing backpropagation on both performance and robustness metrics? Intuition can be gained by simply considering the functional form of $\mathcal{R}_{\text{WM}}$, which can become *arbitrarily* negative even for fixed values of the forward weights. $\mathcal{R}_{\text{WM}}$ is a combination of a primitive which depends on the input ($\mathcal{P}^{\text{amp}}$) and a primitive which is independent of the input ($\mathcal{P}^{\text{decay}}$). Because of this, the primitives of weight mirror and their gradients may operate at different scales and careful metaparameter tuning must be done to balance their effects. This instability can be made precise by considering the dynamical system given by the symmetrized gradient flow on $\mathcal{R}_{\text{WM}}$ at a given layer l.

In the following analysis we ignore non-linearities, include weight decay on the forward weights, set $\alpha = \beta$, and consider the gradient with respect to both the forward and backward weights. When the weights, w_l and b_l, and input, x_l, are all scalar values, the gradient flow gives rise to the dynamical system

$$\frac{\partial}{\partial t}\begin{bmatrix} w_l \\ b_l \end{bmatrix} = -A\begin{bmatrix} w_l \\ b_l \end{bmatrix}, \tag{1}$$

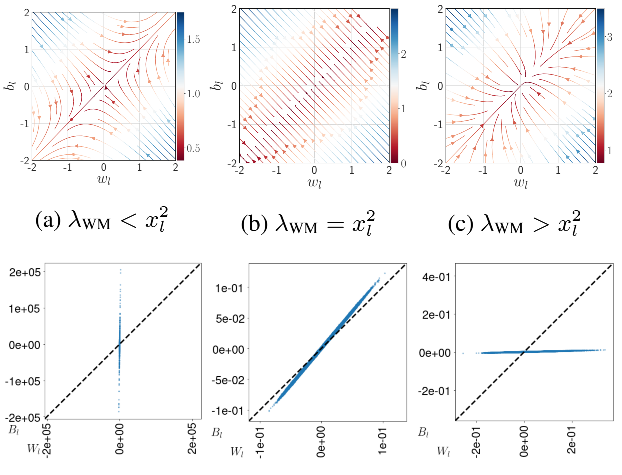

(a) $\lambda_{\text{WM}} < x_l^2$ (b) $\lambda_{\text{WM}} = x_l^2$ (c) $\lambda_{\text{WM}} > x_l^2$

(d) Conv 1 (e) Conv 16 (f) Dense

Figure 2. **Unstable dynamics (a-c).** Symmetrized gradient flow on $\mathcal{R}_{\text{WM}}$ at layer l with scalar weights and $x_l = 1$. The color and arrow indicate respectively the magnitude and direction of the flow. **Empirical instability (d-f).** Weight scatter plots for the first convolution, an intermediate convolution and the final dense layer of a ResNet-18 model trained with weight mirror for five epochs. Each dot represents an element in layer l's weight matrix and its (x, y) location corresponds to its forward and backward weight values, $(W_l^{(i,j)}, B_l^{(j,i)})$. The dotted diagonal line shows perfect weight symmetry, as is the case in backpropagation. Different layers demonstrate one of the the three dynamics outlined by the gradient flow analysis in §4: diverging, stable, and collapsing backward weights.

where A is an indefinite matrix (see Appendix D.1 for details.) A can be diagonally decomposed by the eigenbasis $\{u, v\}$, where u spans the symmetric component and v spans the skew-symmetric component of any realization of the weight vector $\begin{bmatrix} w_l & b_l \end{bmatrix}^\intercal$. Under this basis, the dynamical system decouples into a system of ODEs governed by the eigenvalues of A. The eigenvalue associated with the skew-symmetric eigenvector v is strictly positive, implying that this component decays exponentially to zero. However, for the symmetric eigenvector u, the sign of the corresponding eigenvalue depends on the relationship between λ_{WM} and x_l^2. When $\lambda_{\text{WM}} > x_l^2$, the eigenvalue is positive and the symmetric component decays to zero (i.e. too much regularization). When $\lambda_{\text{WM}} < x_l^2$, the eigenvalue is negative and the symmetric component exponentially grows (i.e. too little regularization). Only when $\lambda_{\text{WM}} = x_l^2$ is the eigenvalue zero and the symmetric component stable. These various dynamics are shown in Fig. 2.

This analysis suggests that the sensitivity of weight mirror is not due to the misalignment of the forward and backward weights, but rather due to the stability of the symmetric component throughout training. Empirically, we find that this is true. In Fig. 2, we show a scatter plot of the backward and forward weights at three layers of a ResNet-18 model trained with weight mirror. At each layer there exists a linear relationship between the weights, suggesting that the backward weights have aligned to the forward weights up to magnitude. Despite being initialized with similar magnitudes, at the first layer the backward weights have grown orders larger, at the last layer the backward weights have decayed orders smaller, and at only one intermediate layer were the backward weights comparable to the forward weights, implying symmetry.

This analysis also clarifies the stabilizing role of Gaussian noise, which was found to be essential to weight mirror's performance gains over feedback alignment (Akrout et al., 2019). Specifically, when the layer input $x_l \sim N\left(0, \sigma^2\right)$ and $\sigma^2 = \lambda_{\text{WM}}$, then $x_l^2 \approx \lambda_{\text{WM}}$, implying the dynamical system in equation (1) is stable.

Strategies for Reducing Instability. Given the above analysis, can we identify further strategies for reducing instability during learning beyond the use of Gaussian noise?

Adaptive Optimization. One option is to use an adaptive learning rule strategy, such as Adam (Kingma & Ba, 2014). An adaptive learning rate keeps an exponentially decaying moving average of past gradients, allowing for more effective optimization of the alignment regularizer even in the presence of exploding or vanishing gradients.

Local Stabilizing Operations. A second option to improve stability is to consider local layer-wise operations to the backward path such as choice of non-linear activation functions, batch centering, feature centering, and feature normalization. The use of these operations is largely inspired by Batch Normalization (Ioffe & Szegedy, 2015) and Layer Normalization (Ba et al., 2016) which have been observed to stabilize learning dynamics. The primary improvement that these normalizations allow for is the further conditioning of the covariance matrix at each layer's input, building on the benefits of using Gaussian noise. In order to keep the learning rule fully local, we use these normalizations, which unlike Batch and Layer Normalization, do not add any additional learnable parameters.

The Information Alignment (IA) Learning Rule. There is a third option for improving stability that involves modifying the local learning rule itself.

Without decay, the update given by weight mirror, $\Delta B_l = \eta x_l x_{l+1}^\intercal$, is Hebbian. This update, like all purely Hebbian learning rules, is unstable and can result in the norm of B_l diverging. This can be mitigated by weight decay, as is done in Akrout et al. (2019). However, an alternative strategy to dealing with the instability of a Hebbian update was given by Oja (1982) in his analysis of learning rules for linear neuron models. In the spirit of that analysis, assume that we can normalize the backward weight after each Hebbian update such that

$$B_l^{(t+1)} = \frac{B_l^{(t)} + \eta x_l x_{l+1}^\intercal}{||B_l^{(t)} + \eta x_l x_{l+1}^\intercal||},$$

and in particular $||B_l^{(t)}|| = 1$ at all time t. Then, for small learning rates η, the right side can be expanded as a power series in η, such that

$$B_l^{(t+1)} = B_l^{(t)} + \eta \left(x_l x_{l+1}^\intercal - B_l^{(t)} x_l^\intercal B_l^{(t)} x_{l+1} \right) + O(\eta^2).$$

Ignoring the $O(\eta^2)$ term gives the non-linear update

$$\Delta B_l = \eta \left(x_l x_{l+1}^\intercal - B_l x_l^\intercal B_l x_{l+1} \right).$$

If we assume $x_l^\intercal B_l = x_{l+1}$ and B_l is a column vector rather than a matrix, then by Table 1, this is approximately the update given by the null primitive introduced in §3.1.

Thus motivated, we define **Information Alignment (IA)** as the local learning rule defined by adding a (weighted) null primitive to the other two local primitives already present in the weight mirror rule. That is, the layer-wise regularization function

$$\mathcal{R}_{\text{IA}} = \sum_{l \in \text{layers}} \alpha \mathcal{P}_l^{\text{amp}} + \beta \mathcal{P}_l^{\text{decay}} + \gamma \mathcal{P}_l^{\text{null}}.$$

In the specific setting when $x_{l+1} = W_l x_l$ and $\alpha = \gamma$, then the gradient of $\mathcal{R}_{\text{IA}}$ is proportional to the gradient with respect to B_l of $\frac{1}{2}||x_l - B_l W_l x_l||^2 + \frac{\beta}{2}\left(||W_l||^2 + ||B_l||^2\right)$, a quadratically regularized linear autoencoder[3]. As shown in Kunin et al. (2019), all critical points of a quadratically regularized linear autoencoder attain symmetry of the encoder and decoder.

Empirical Results. To evaluate the three strategies for stabilizing local weight updates, we performed a neural architecture search implementing all three strategies, again using TPE. This search optimized for Top-1 ImageNet validation performance with the ResNet-18 architecture, comprising a total of 628 distinct settings. We found that validation performance increased significantly, with the optimal learning rule $\mathcal{R}_{\text{IA}}^{\text{TPE}}$, attaining 67.93% top-1 accuracy (Table 3). More importantly, we also found that the parameter robustness of $\mathcal{R}_{\text{IA}}^{\text{TPE}}$ is dramatically improved as compared to weight mirror (Fig. 3, orange line), nearly equaling the parameter robustness of backpropagation across a variety of deeper architectures. Critically, this improvement was achieved not by directly optimizing for robustness across architectures, but simply by finding a parameter setting that achieved high task performance on one architecture.

[3]In this setting, the resulting learning rule is a member of the target propagation framework introduced in §2.

Learning Rule	Top-1 Val Accuracy	Top-5 Val Accuracy
$\mathcal{R}_{\text{WM}}$	63.5%	85.16%
$\mathcal{R}_{\text{WM}}^{\text{TPE}}$	64.07%	85.47%
$\mathcal{R}_{\text{WM+AD}}^{\text{TPE}}$	64.40%	85.53%
$\mathcal{R}_{\text{WM+AD+OPS}}^{\text{TPE}}$	63.41%	84.83%
$\mathcal{R}_{\text{IA}}^{\text{TPE}}$	**67.93%**	**88.09%**
Backprop.	70.06%	89.14%

Table 3. **Performance of local learning rules with ResNet-18 on ImageNet.** $\mathcal{R}_{\text{WM}}$ is weight mirror as described in Akrout et al. (2019), $\mathcal{R}_{\text{WM}}^{\text{TPE}}$ is weight mirror with learning metaparameters chosen through an optimization procedure. $\mathcal{R}_{\text{WM+AD}}^{\text{TPE}}$ is weight mirror with an adaptive optimizer. $\mathcal{R}_{\text{WM+AD+OPS}}^{\text{TPE}}$ involves the addition of stabilizing operations to the network architecture. The best local learning rule, $\mathcal{R}_{\text{IA}}^{\text{TPE}}$, additionally involves the null primitive. For details on metaparameters for each local rule, see Appendix B.1.

To assess the importance of each strategy type in achieving this result, we also performed several ablation studies, involving neural architecture searches using only various subsets of the stabilization strategies (see Appendix B.1.3 for details). Using just the adaptive optimizer while otherwise optimizing the weight mirror metaparameters yielded the learning rule $\mathcal{R}_{\text{WM+AD}}^{\text{TPE}}$, while adding stabilizing layer-wise operations yielded the learning rule $\mathcal{R}_{\text{WM+AD+OPS}}^{\text{TPE}}$ (Table 3). We found that while the top-1 performance of these ablated learning rules was not better for the ResNet-18 architecture than the weight-mirror baseline, each of the strategies did individually contribute significantly to improved parameter robustness (Fig. 3, red and green lines).

Taken together, these results indicate that the regularization framework allows the formulation of local learning rules with substantially improved performance and, especially, metaparameter robustness characteristics. Moreover, these improvements are well-motivated by mathematical analysis that indicates how to target better circuit structure via improved learning stability.

5. Non-Local Learning Rules

While our best local learning rule is substantially improved as compared to previous alternatives, it still does not quite match backpropagation, either in terms of performance or metaparameter stability over widely different architectures (see the gap between blue and orange lines in Fig. 3). We next introduce two novel non-local learning rules that entirely eliminate this gap.

Symmetric Alignment (SA) is defined by the layer-wise regularization function

$$\mathcal{R}_{\text{SA}} = \sum_{l \in \text{layers}} \alpha \mathcal{P}_l^{\text{self}} + \beta \mathcal{P}_l^{\text{decay}}.$$

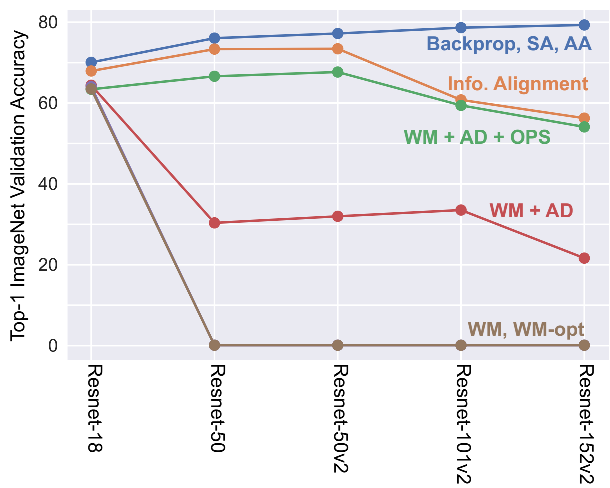

Figure 3. **Performance of local and non-local rules across architectures.** We fixed the categorical and continuous metaparameters for ResNet-18 and applied them directly to deeper and different ResNet variants (e.g. v2). A performance of 0.001 indicates the alignment loss became NaN within the first thousand steps of training. Our local rule Information Alignment (IA) consistently outperforms the other *local* alternatives across architectures, despite not being optimized for these architectures. The non-local rules, Symmetric Alignment (SA) and Activation Alignment (AA), consistently perform as well as backpropagation.

When $\alpha = \beta$, then the gradient of $\mathcal{R}_{\text{SA}}$ is proportional to the gradient with respect to B_l of $\frac{1}{2}||W_l - B_l^{\intercal}||^2$, which encourages symmetry of the weights.

Activation Alignment (AA) is defined by the layer-wise regularization function

$$\mathcal{R}_{\text{AA}} = \sum_{l \in \text{layers}} \alpha \mathcal{P}_l^{\text{amp}} + \beta \mathcal{P}_l^{\text{sparse}}.$$

When $x_{l+1} = W_l x_l$ and $\alpha = \beta$, then the gradient of $\mathcal{R}_{\text{AA}}$ is proportional to the gradient with respect to B_l of $\frac{1}{2}||W_l x_l - B_l^{\intercal} x_l||^2$, which encourages alignment of the activations.

Both SA and AA give rise to dynamics that encourage the backward weights to become transposes of their forward counterparts. When B_l is the transpose of W_l for all layers l then the updates generated by the backward pass are the exact gradients of $\mathcal{J}$. It follows intuitively that throughout training the pseudogradients given by these learning rules might converge to better approximations of the exact gradients of $\mathcal{J}$, leading to improved learning. Further, in the context of the analysis in equation (1), the matrix A associated with SA and AA is positive semi-definite, and unlike the case of weight mirror, the eigenvalue associated with the symmetric eigenvector u is zero, implying stability of the symmetric component.

While weight mirror and Information Alignment introduce dynamics that implicitly encourage symmetry of the forward

Model	Backprop.	Symmetric	Activation
ResNet-18	70.06%	69.84%	69.98%
ResNet-50	76.05%	76.29%	75.75%
ResNet-50v2	77.21%	77.18%	76.67%
ResNet-101v2	78.64%	78.74%	78.35%
ResNet-152v2	79.31%	79.15%	78.98%

Table 4. **Symmetric and Activation Alignment consistently match backpropagation.** Top-1 validation accuracies on ImageNet for each model class and non-local learning rule, compared to backpropagation.

and backward weights, the dynamics introduced by SA and AA encourage this property explicitly.

Despite not having the desirable locality property, we show that SA and AA perform well empirically in the weight-decoupled regularization framework — meaning that they *do* relieve the need for exact weight symmetry. As we will discuss, this may make it possible to find plausible biophysical mechanisms by which they might be implemented.

Parameter Robustness of Non-Local Learning Rules. To assess the robustness of SA and AA, we trained ResNet-18 models with standard 224-sized ImageNet images (training details can be found in Appendix B.2). Without any metaparameter tuning, SA and AA were able to match backpropagation in performance. Importantly, for SA we did not need to employ any specialized or adaptive learning schedule involving alternating modes of learning, as was required for all the local rules. However, for AA we did find it necessary to use an adaptive optimizer when minimizing $\mathcal{R}_{\text{AA}}$, potentially due to the fact that it appears to align less exactly than SA (see Fig. S3). We trained deeper ResNet-50, 101, and 152 models (He et al., 2016) with larger 299-sized ImageNet images. As can be seen in Table 4, both SA and AA maintain consistent performance with backpropagation despite changes in image size and increasing depth of network architecture, demonstrating their robustness as a credit assignment strategies.

Weight Estimation, Neural Plausibility, and Noise Robustness. Though SA is non-local, it does avoid the need for instantaneous weight transport — as is shown simply by the fact that it optimizes effectively in the framework of decoupled forward-backward weight updates, where alignment can only arise over time due to the structure of the regularization circuit rather than instantaneously by *fiat* at each timepoint. Because of this key difference, it may be possible to find plausible biological implementations for SA, operating on a principle of iterative "weight estimation" in place of the implausible idea of instantaneous weight transport.

By "weight estimation" we mean any process that can mea-

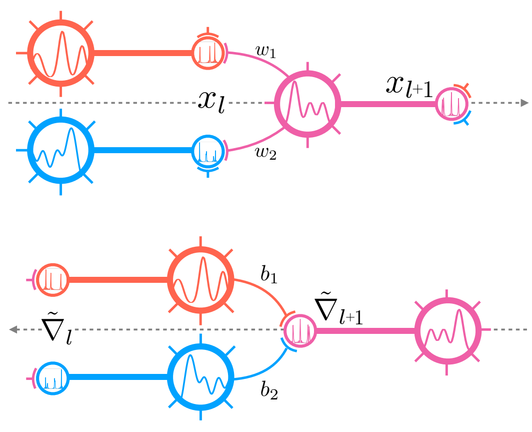

(a) Neural Circuit Diagram

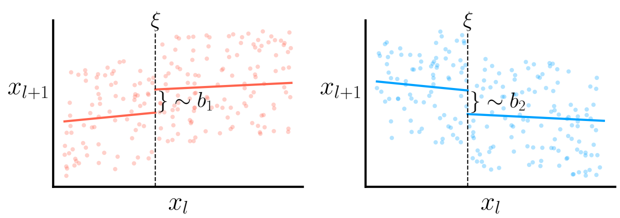

(b) Regression Discontinuity Design

Figure 4. **Weight estimation.** (a) The notational diagram, as shown in Fig. 1, is mapped into a neural circuit. The top and bottom circuits represent the forward and backward paths respectively. Large circles represent the soma of a neuron, thick edges the axon, small circles the axon terminal, and thin edges the dendrites. Dendrites corresponding to the lateral pathways between the circuits are omitted. (b) A mechanism such as regression discontinuity design, as explained by Lansdell & Kording (2019) and Guerguiev et al. (2019), could be used independently at each neuron to do weight estimation by quantifying the causal effect of x_l on x_{l+1}.

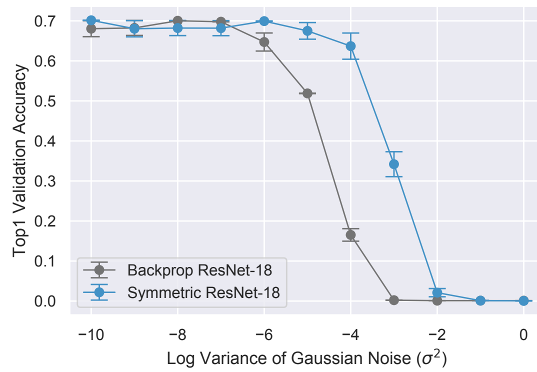

(a) ResNet-18

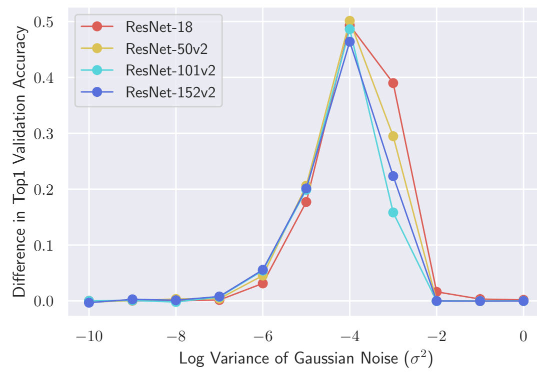

(b) Deeper Models

Figure 5. **Symmetric Alignment is more robust to noisy updates than backpropagation.** (a) Symmetric Alignment is more robust than backpropagation to increasing levels of Gaussian noise added to its updates for ResNet-18. (b) Symmetric Alignment maintains this robustness for deeper models. See Appendix B.3 for more details and similar experiments with Activation Alignment.

sure changes in post-synaptic activity relative to varying synaptic input, thereby providing a temporal estimate of the synaptic strengths. Prior work has shown how noisy perturbations in the presence of spiking discontinuities (Lansdell & Kording, 2019) could provide neural mechanisms for weight estimation, as depicted in Fig. 4. In particular, Guerguiev et al. (2019) present a spiking-level mechanism for estimating forward weights from noisy dendritic measurements of the implied effect of those weights on activation changes. This idea, borrowed from the econometrics literature, is known as regression discontinuity design (Imbens & Lemieux, 2008). This is essentially a form of iterative weight estimation, and is used in Guerguiev et al. (2019) for minimizing a term that is mathematically equivalent to $\mathcal{P}^{\text{self}}$. Guerguiev et al. (2019) demonstrate that this weight estimation mechanism works empirically for small-scale networks.

Our performance and robustness results above for SA can be interpreted as providing evidence that a rate-coded version of weight estimation scales effectively to training deep networks on large-scale tasks. However, there remains a gap between what we have shown at the rate-code level and the spike level, at which the weight estimation mechanism operates. Truly showing that weight estimation could work at scale would involve being able to train deep spiking neural networks, an unsolved problem that is beyond the scope of this work. One key difference between any weight estimation process at the rate-code and spike levels is that the latter will be inherently noisier due to statistical fluctuations in whatever local measurement process is invoked — e.g. in the Guerguiev et al. (2019) mechanism, the noise in computing the regression discontinuity.

As a proxy to better determine if our conclusions about the scalable robustness of rate-coded SA are likely to apply to spiking-level equivalents, we model this uncertainty by adding Gaussian noise to the backward updates during learning. To the extent that rate-coded SA is robust to such noise,

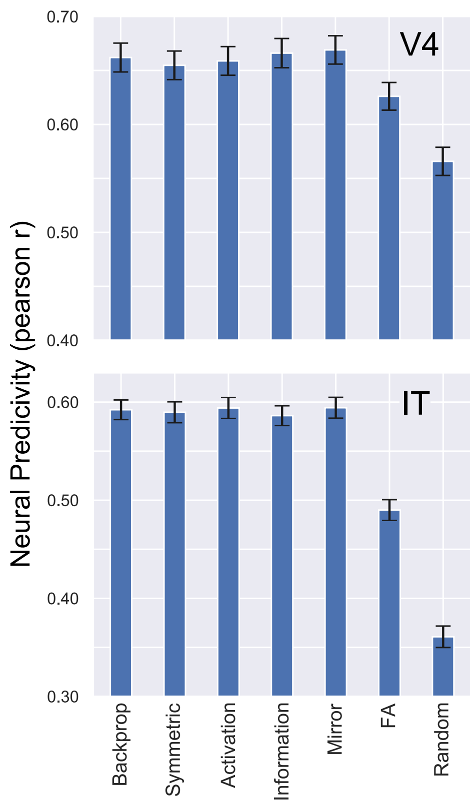

Figure 6. **Neural fits to temporally-averaged V4 and IT responses.** Neural fits to V4 (top) and IT (bottom) time-averaged responses (Majaj et al., 2015), using a 25 component PLS mapping on a ResNet-18. The median (across neurons) Pearson correlation over images, with standard error of mean (across neurons) denoting the error bars. "Random" refers to a ResNet-18 architecture at initialization. For details, see Appendix B.5.

the more likely it is that a spiking-based implementation will have the performance and parameter robustness characteristics of the rate-coded version. Specifically, we modify the update rule as follows:

$$\Delta\theta_b \propto \nabla\mathcal{R} + \mathcal{N}(0, \sigma^2), \qquad \Delta\theta_f \propto \widetilde{\nabla}\mathcal{J}.$$

As shown in Fig. 5, the performance of SA is very robust to noisy updates for training ResNet-18. In fact, for comparison we also train backpropagation with Gaussian noise added to its gradients, $\Delta\theta \propto \nabla\mathcal{J} + \mathcal{N}(0, \sigma^2)$, and find that SA is substantially *more* robust than backpropagation. For deeper models, SA maintains this robustness, implying that pseudogradients generated by backward weights with noisy updates leads to more robust learning than using equivalently noisy gradients directly.

6. Discussion

In this work, we present a unifying framework that allows for the systematic identification of robust and scalable alternatives to backpropagation. We obtain, through large-scale searches, a local learning rule that transfers more robustly across architectures than previous local alternatives. Nonetheless, a performance and robustness gap persists with backpropagation. We formulate non-local learning rules that achieve competitive performance with backpropagation, requiring almost no metaparameter tuning and are robust to noisy updates. Taken together, our findings suggest that there are two routes towards the discovery of robust, scalable, and neurally plausible credit assignment without weight symmetry.

The first route involves further improving local rules. We found that the local operations and regularization primitives that allow for improved approximation of non-local rules perform better and are much more stable. If the analyses that inspired this improvement could be refined, perhaps further stability could be obtained. To aid in this exploration going forward, we have written an open-source TensorFlow library[4], allowing others to train arbitrary network architectures and learning rules at scale, distributed across multiple GPU or TPU workers. The second route involves the further refinement and characterization of scalable biological implementations of weight estimation mechanisms for Symmetric or Activation Alignment, as Guerguiev et al. (2019) initiate.

Given these two routes towards neurally-plausible credit assignment without weight symmetry, how would we use neuroscience data to adjudicate between them? It would be convenient if functional response data in a "fully trained" adult animal showed a signature of the underlying learning rule, without having to directly measure synaptic weights during learning. Such data have been very effective in identifying good models of the primate ventral visual pathway (Majaj et al., 2015; Yamins et al., 2014). As an initial investigation of this idea, we compared the activation patterns generated by networks trained with each local and non-local learning rule explored here, to neural response data from several macaque visual cortical areas, using a regression procedure similar to that in Yamins et al. (2014). As shown in Fig. 6, we found that, with the exception of the very poorly performing feedback alignment rule, all the reasonably effective learning rules achieve similar V4 and IT neural response predictivity, and in fact match that of the network learned via backpropagation. Such a result suggests the interesting possibility that the functional response signatures in an already well-learned neural representation may be relatively independent of which learning rule created them. Perhaps unsurprisingly, the question of identifying the operation of learning rules in an *in vivo* neural circuit will likely require the deployment of more sophisticated neuroscience techniques.

[4] `https://github.com/neuroailab/neural-alignment`

Acknowledgements

We thank the Stanford Data Science Scholars program (DK), the Burroughs Wellcome (DY), Simons (SG, DY) and James S. McDonnell (DY) foundations, NSF career awards (SG, DY), and the NSF Robust Intelligence program, for support. We thank the Google TensorFlow Research Cloud (TFRC) team for providing TPU resources for this project.

References

Akrout, M., Wilson, C., Humphreys, P. C., Lillicrap, T., and Tweed, D. Deep Learning without Weight Transport. *arXiv:1904.05391 [cs, stat]*, April 2019. URL http://arxiv.org/abs/1904.05391. arXiv: 1904.05391.

Ba, J. L., Kiros, J. R., and Hinton, G. E. Layer normalization. *arXiv preprint arXiv:1607.06450*, 2016.

Baldi, P., Sadowski, P., and Lu, Z. Learning in the machine: Random backpropagation and the deep learning channel. *Artificial Intelligence*, 260:1–35, 2018. doi: 10.1016/j.artint.2018.03.003.

Bartunov, S., Santoro, A., Richards, B., Marris, L., Hinton, G. E., and Lillicrap, T. Assessing the Scalability of Biologically-Motivated Deep Learning Algorithms and Architectures. In Bengio, S., Wallach, H., Larochelle, H., Grauman, K., Cesa-Bianchi, N., and Garnett, R. (eds.), *Advances in Neural Information Processing Systems 31*, pp. 9368–9378. Curran Associates, Inc., 2018. URL http://papers.nips.cc/paper/8148-assessing-the-scalability-of-biologically-motivated-deep-learning-algorithms-and-architectures.pdf.

Bengio, Y. How Auto-Encoders Could Provide Credit Assignment in Deep Networks via Target Propagation. *ArXiv*, abs/1407.7906, 2014.

Bengio, Y., Mesnard, T., Fischer, A., Zhang, S., and Wu, Y. STDP-Compatible Approximation of Backpropagation in an Energy-Based Model. *Neural Computation*, 29(3):555–577, 2017. doi: 10.1162/NECO_a_00934. URL https://doi.org/10.1162/NECO_a_00934. PMID: 28095200.

Bergstra, J. S., Bardenet, R., Bengio, Y., and Kégl, B. Algorithms for hyper-parameter optimization. In *Advances in neural information processing systems*, pp. 2546–2554, 2011.

Buchlovsky, P., Budden, D., Grewe, D., Jones, C., Aslanides, J., Besse, F., Brock, A., Clark, A., Colmenarejo, S. G., Pope, A., et al. Tf-replicator: Distributed machine learning for researchers. *arXiv preprint arXiv:1902.00465*, 2019.

Cadena, S. A., Denfield, G. H., Walker, E. Y., Gatys, L. A., Tolias, A. S., Bethge, M., and Ecker, A. S. Deep convolutional models improve predictions of macaque v1 responses to natural images. *PLoS computational biology*, 15(4):e1006897, 2019.

Crick, F. The recent excitement about neural networks. *Nature*, 337:129–132, 1989. doi: 10.1038/337129a0.

Grossberg, S. Competitive Learning: From Interactive Activation to Adaptive Resonance. *Cognitive Science*, 11: 23–63, 1987.

Guerguiev, J., Lillicrap, T. P., and Richards, B. A. Towards deep learning with segregated dendrites. *eLife*, 6, 2017. doi: 10.7554/eLife.22901.

Guerguiev, J., Kording, K. P., and Richards, B. A. Spike-based causal inference for weight alignment. *arXiv:1910.01689 [cs, q-bio]*, October 2019. URL http://arxiv.org/abs/1910.01689. arXiv: 1910.01689.

He, K., Zhang, X., Ren, S., and Sun, J. Deep Residual Learning for Image Recognition. In *2016 IEEE Conference on Computer Vision and Pattern Recognition (CVPR)*, pp. 770–778, June 2016. doi: 10.1109/CVPR.2016.90. ISSN: 1063-6919.

Imbens, G. W. and Lemieux, T. Regression discontinuity designs: A guide to practice. *Journal of econometrics*, 142(2):615–635, 2008.

Ioffe, S. and Szegedy, C. Batch normalization: Accelerating deep network training by reducing internal covariate shift. *arXiv preprint arXiv:1502.03167*, 2015.

Kingma, D. P. and Ba, J. Adam: A method for stochastic optimization. *arXiv preprint arXiv:1412.6980*, 2014.

Kolen, J. and Pollack, J. Backpropagation without weight transport. In *Proceedings of 1994 IEEE International Conference on Neural Networks (ICNN'94)*, volume 3, pp. 1375 – 1380 vol.3, 07 1994. ISBN 0-7803-1901-X. doi: 10.1109/ICNN.1994.374486.

Kunin, D., Bloom, J., Goeva, A., and Seed, C. Loss Landscapes of Regularized Linear Autoencoders. In Chaudhuri, K. and Salakhutdinov, R. (eds.), *Proceedings of the 36th International Conference on Machine Learning*, volume 97 of *Proceedings of Machine Learning Research*, pp. 3560–3569, Long Beach, California, USA, 09–15 Jun 2019. PMLR. URL http://proceedings.mlr.press/v97/kunin19a.html.

Lansdell, B. J. and Kording, K. P. Spiking allows neurons to estimate their causal effect. *bioRxiv*, pp. 253351, 2019.

Lee, D.-H., Zhang, S., Fischer, A., and Bengio, Y. Difference target propagation. In *Joint european conference on machine learning and knowledge discovery in databases*, pp. 498–515. Springer, 2015.

Liao, Q., Leibo, J. Z., and Poggio, T. How Important is Weight Symmetry in Backpropagation? In *Proceedings of the Thirtieth AAAI Conference on Artificial Intelligence*, AAAI'16, pp. 1837–1844. AAAI Press, 2016. URL http://dl.acm.org/citation.cfm?id=3016100.3016156.

Lillicrap, T. P., Cownden, D., Tweed, D. B., and Akerman, C. J. Random synaptic feedback weights support error backpropagation for deep learning. *Nature Communications*, 7:13276, November 2016. ISSN 2041-1723. doi: 10.1038/ncomms13276. URL https://www.nature.com/articles/ncomms13276.

Majaj, N. J., Hong, H., Solomon, E. A., and DiCarlo, J. J. Simple Learned Weighted Sums of Inferior Temporal Neuronal Firing Rates Accurately Predict Human Core Object Recognition Performance. *The Journal of neuroscience : the official journal of the Society for Neuroscience*, 35:13402–18, 2015 Sep 30 2015. ISSN 1529-2401. doi: 10.1523/JNEUROSCI.5181-14.2015.

Moskovitz, T. H., Litwin-Kumar, A., and Abbott, L. F. Feedback alignment in deep convolutional networks. *CoRR*, abs/1812.06488, 2018. URL http://arxiv.org/abs/1812.06488.

Nøkland, A. Direct Feedback Alignment Provides Learning in Deep Neural Networks. In *Advances in neural information processing systems*, pp. 1037–1045, 2016.

Oja, E. A simplified neuron model as a principal component analyzer. *E. J. Math. Biology*, 15(3):267 – 273, 1982. doi: 10.1007/BF00275687.

Rumelhart, D. E., Hinton, G. E., and Williams, R. J. Learning representations by back-propagating errors. *Nature*, 323:533–536, October 1986. doi: 10.1038/323533a0.

Sacramento, J. a., Ponte Costa, R., Bengio, Y., and Senn, W. Dendritic cortical microcircuits approximate the backpropagation algorithm. In Bengio, S., Wallach, H., Larochelle, H., Grauman, K., Cesa-Bianchi, N., and Garnett, R. (eds.), *Advances in Neural Information Processing Systems 31*, pp. 8721–8732. Curran Associates, Inc., 2018. URL http://papers.nips.cc/paper/8089-dendritic-cortical-microcircuits-approximate-the-backpropagation-algorithm.pdf.

Saxe, A., Mcclelland, J., and Ganguli, S. Exact solutions to the nonlinear dynamics of learning in deep linear neural networks. *arXiv preprint arXiv:1312.6120*, 12 2013.

Scellier, B. and Bengio, Y. Equilibrium Propagation: Bridging the Gap between Energy-Based Models and Backpropagation. *Frontiers in Computational Neuroscience*, 11:24, 2017. ISSN 1662-5188. doi: 10.3389/fncom.2017.00024. URL https://www.frontiersin.org/article/10.3389/fncom.2017.00024.

Whittington, J. C. R. and Bogacz, R. An Approximation of the Error Backpropagation Algorithm in a Predictive Coding Network with Local Hebbian Synaptic Plasticity. *Neural computation*, 29(5):1229–1262, 2017.

Xiao, W., Chen, H., Liao, Q., and Poggio, T. Biologically-Plausible Learning Algorithms Can Scale to Large Datasets. In *International Conference on Learning Representations*, 2019. URL https://openreview.net/forum?id=SygvZ209F7.

Xie, X. and Seung, H. Equivalence of Backpropagation and Contrastive Hebbian Learning in a Layered Network. *Neural computation*, 15:441–54, 03 2003. doi: 10.1162/089976603762552988.

Yamins, D. L., Hong, H., Cadieu, C. F., Solomon, E. A., Seibert, D., and DiCarlo, J. J. Performance-optimized hierarchical models predict neural responses in higher visual cortex. *Proceedings of the National Academy of Sciences*, 111(23):8619–8624, 2014.